



II Fabre Conference – Existing bridges, viaducts and tunnels: research, innovation and applications (FABRE24)

Vision-based approach for the static and dynamic monitoring of bridges

Federico Ponsi^a, Edoardo Buoli^b, Ghita Eslami Varzaneh^b, Elisa Bassoli^{b,*}, Bruno Briseghella^{b,c}, Loris Vincenzi^b

^aDepartment of Civil, Chemical, Environmental, and Materials Engineering, University of Bologna, Bologna 40126, Italy

^bDepartment of Engineering “Enzo Ferrari”, University of Modena and Reggio Emilia, Modena, 41125, Italy

^cCollege of Civil Engineering, Fuzhou University, Fuzhou, 350108, China

Abstract

Structural Health Monitoring (SHM) is one of the main approaches to deal with damage identification in existing bridges. Static information together with structure modal properties allow to prevent collapses, detect damage also in the early stage, and plan maintenance works based on the bridge condition. Measurement systems are traditionally composed of a network of sensors directly installed on the structure. Despite the large diffusion of these systems, the expensive and time-consuming installation of sensors and acquisition system makes their use not always feasible. A promising approach for the characterization of bridge dynamic behavior is represented by computer vision-based techniques, which require the sole installation of one or more cameras outside the structure, along with some targets on it when necessary. This approach is totally non-invasive, low-cost and enables the direct measurement of structural displacements, providing useful and direct information about the operational conditions and possible permanent deformations. With the aim of investigating the potential of vision-based techniques for the dynamic monitoring of structures, this paper presents preliminary results of dynamic tests performed on a steel footbridge. Structural vibrations caused by a jumping pedestrian were measured from a camera placed at the riverbed as well as by an accelerometer-based monitoring system installed for validation purposes. The post-processing of video recordings is here presented and discussed, with particular emphasis on the impact of target shape and camera shaking.

© 2024 The Authors. Published by Elsevier B.V.

This is an open access article under the CC BY-NC-ND license (<https://creativecommons.org/licenses/by-nc-nd/4.0>)

Peer-review under responsibility of Scientific Board Members

* Corresponding author. Tel.: +39-059-205-6337.

E-mail address: elisa.bassoli@unimore.it

Keywords: vision-based health monitoring; target shape; camera movements; steel footbridge.

1. Introduction

Vibration monitoring plays a key role in many structural applications, ranging from system identification and model updating (Ranieri et al., 2020; Ponsi et al., 2022) to health assessment and damage detection (Comanducci et al., 2016; Ponsi et al., 2023). Despite the consolidation of traditional monitoring based on dense wired-sensor networks, the engineering community focus is increasingly shifting towards non-contact structural monitoring. Indeed, the use of remote technologies saves the complicated task of wiring, drastically reducing installation efforts, set-up time, test costs and traffic disruptions. Contactless technologies available for civil monitoring purposes include, for instance, global navigation satellite systems (GNSS) (Poluzzi et al., 2019), satellite remote sensing (Bassoli et al., 2023), terrestrial radar interferometry (Castagnetti et al., 2019; Guerzoni et al. 2023), and vision-based techniques (Fradelos et al., 2020). Among them, the latter are the only type of remote sensing with the potential to overcome the dependence on expensive industrial products (Xu et al., 2019), showing great potentialities even with consumer-grade instrumentations. All this thanks to the development of low-cost technologies featured by high resolution and high frame rates, in favor of a promising accuracy for large-scale structures in the dynamic field. Moreover, the approach is also applicable to detect long-term static displacements (Lee et al., 2020), and is able to reach high accuracies with even more limited frame rates by averaging the displacements over a large frame window. Beyond the business side, other advantages of vision-based methods are the direct evaluation of displacements (without the need for a double integration of accelerations) and the multipoint monitoring capacity of a single video-camera. In addition, only distinctive targets placed at locations of interest are required, which might be artificial patterns specifically installed for the testing or peculiar elements of the structure itself, such as evident details, corners, or bolts (Dong et al., 2020). Physical installations are thus substantially reduced or even eliminated, which is extremely attractive when the structure is not easily or safely accessible as well as if it is part of the cultural heritage.

Featured by all these benefits compared with traditional monitoring, vision-based techniques are in recent years gaining increasing attention in the civil research field. Latest applications are comprehensively reviewed in the works of Spencer et al. (2019), Dong and Catbas (2020), and Zona (2021), comprising tests on bridges (Feng and Feng, 2017; Chen et al., 2018) and footbridges (Xu et al., 2018; Lydon et al., 2019). Besides the practical advantages, the accuracy of measurements is not solely dependent on the video camera technical specifications. In addition to the hardware intrinsic performance, equally delicate are the perspective adjustment and scaling, relevant to the software process. Moreover, other critical aspects widely recognized as sources of errors and uncertainties are those related to the environmental condition, such as vibrations of the camera or its support due to user intervention or wind, variable weather and ambient light, non-uniform air refraction caused by temperature differences between the camera and the object being monitored. Different studies on the assessment of environmental uncertainties in vision-based monitoring can be found in literature (Ye et al., 2016), mostly through theoretical analyses and laboratory testing (Zona, 2021). The influence of external factors on the accuracy of on-site tests is, however, still not well clear and under investigation. This is also due to the lack of outdoor full-scale tests, given that vision-based techniques have only recently been adapted to large-scale civil constructions.

In this context, the main objective of this research activity is to test the potential and the criticisms of a real-scale on-site dynamic vision-based monitoring. The case study consists of a steel deformable footbridge built in Modena (Italy), on which targets with different geometries have been installed, along with a traditional accelerometer network that serves as a validation tool. Section 2 describes the monitoring campaign, during which videos were acquired under pedestrian jumping condition. Afterwards, the designed vision-based algorithms (presented in Section 3) are adopted to post-process video recordings. The idea is quite simple in its principle, as it consists in detecting the position of targets within each video-frame to consequently reconstruct the dynamic motion of the bridge itself. Two different target tracking techniques are tested. The first is developed by the authors and deals with prefixed target, while the second is a feature point matching technique proposed in literature (Lydon et al., 2019) that exploits bolts as key-point targets. Preliminary results are discussed in Section 4. More specifically, the attention is herein focused on the impact of camera shaking and on the accuracy of vision-based displacements depending on the algorithm type and target geometry. Finally, conclusions and future perspectives are drawn in Section 5.

2. Case study and monitoring campaign

The case study is a 3D truss-girder steel footbridge located across the Panaro river, in Modena, Italy (see Fig. 1a). Slender and lightweight, the footbridge is highly deformable and extremely sensitive to dynamic vibrations induced by pedestrians, cyclists, and wind. The box cross section measures 3.00 x 3.20 m, composed of truss girders with hollow tubular section elements. The total length of the structure is 160 m, subdivided into three spans of 45 m, 70 m and 45 m. Four footbridge cross sections belonging to the central span are equipped to be monitored, i.e., midspan, quarter, three-eighths, and a section near the piers. Targets are installed on each of the above-mentioned sections. Fig. 1c shows an example of the targets installed on the structure, composed two different pattern geometries.

The instrumentation consists in a Nikon D7500 placed outside the structure on the dry riverbed, viewing the footbridge in longitudinal perspective. Videos are recorded in 4K resolution at 30 FPS (frames per second). To prevent camera shaking due to user manual intervention, a remote controller is adopted to start-and-stop video acquisitions. Moreover, to be capable of quantifying and removing camera vibrations caused by environmental factors, other four targets are placed on the ground. Indeed, such fixed targets can be exploited as reference stationary objects for image stabilization. Besides, a traditional monitoring system composed of 4 biaxial MEMS accelerometers (Guidorzi et al., 2010) is installed for validation purposes. Sensors are placed at the examined footbridge sections, with sampling frequency set at 80 Hz.

During the monitoring campaign, footbridge vibrations are acquired in forced condition, consisting in a jumping excitation set at 138 BPM (beats per minute) thanks to the use of a metronome. Such a cadence is meant to excite as much as possible the first vertical mode of the footbridge, featured by a natural frequency of 2.32 Hz (value extracted from acceleration responses recorded during preliminary operational tests). The video duration covers some instants prior to the excitation (to measure data noise in ambient condition), the 10 seconds jumping session, and the next two minutes, to also acquire the structural motion attenuation following the forcing.



Fig. 1. (a) Wide view of the footbridge; (b) Detail on the monitoring setup; (c) target employed for the monitoring.

3. Vision-based displacements detection

A video is a sequence of frames visualized at high speed. Assuming that the camera is in a state of rest, the relative difference between the target position in subsequent frames is related to the displacement of the relevant footbridge section over time. The procedures adopted to extract structural displacements from recorded videos are hereinafter illustrated, starting from the developed target tracking algorithms and concluding with a literature feature-point matching technique.

3.1. Developed target tracking algorithms

The designed pre-processing procedure employs the MATLAB Image Processing and Computer Vision Toolboxes (R2022), which allow to import the video, convert truecolor to greyscale, extract frames, remove lens distortion,

manually select the region of interest (ROI), and correct the perspective distortion (only if circle targets are concerned). The lens distortion is removed by correcting the video frames based on the camera parameters resulting from a calibration procedure. The ROI definition is needed since the identification of targets may be complex if operated over the entire frame, due to eventual false detections. However, the ROI must be sufficiently wide to ensure the visibility of the moving target among all the video frames. Perspective distortions are eliminated through homogeneous transformation. Otherwise, depending on the position of the camera, perspective might alter circles into ellipses. During such transformation, the resolution is increased by resampling the ROI with gridded interpolation. In case of the chessboard, instead, perspective deformations do not impact the tracking algorithm, thus the distortion removal is avoided for the sake of simplicity. Anyway, after these operations, the ROI is treated as a pixel matrix. Each pixel is associated with its x and y coordinates (expressed in pixels with respect to the ROI left upper vertex), and with a unique color intensity value in the range $[0, 255]$ (being the image in grayscale). Specifically, an intensity value of 0 represents black, and 255 represents white. When the shape to be detected is not completely contained within a specific number of pixels, the boundary is featured by intermediate $[0, 255]$ intensity values, allowing the object edge detection with sub-pixel accuracy. Basically, the change of intensity value in subsequent pixels (image gradient) is used by the algorithms to identify geometric edges.

As circle detection is concerned, the Circular Hough Transform (CHT) is employed (Atherton and Kerbyson, 1999). The latter is robust in presence of noise, occlusion, and variable illumination, but strictly dependent on the a priori definition of a sensitivity value within the range $[0, 1]$. Too low sensitivity values might not be sufficient to detect all the existent circles, whereas too high values might cause false identifications. Moreover, the optimal sensitivity value might be not the same for all the frames. In light of this, an iterative procedure for automated sensitivity calibration is conceived and implemented. By beforehand imposing the number of circles to be detected, the sensitivity value progressively increases at 0.01 steps until the number of detections matches the requirement. All the frames are thus analyzed, producing a matrix containing, for each frame, the x and y coordinates of the center of each detected circle as well as their radii (all expressed in pixels). The advantage of concentric circles over one alone is that – since all circles are featured by the same center – the frame-by-frame position of the target center can be more accurately estimated by averaging the coordinates of all detected centers. Up to now, coordinates and radii are both expressed in pixels, thus a scaling from pixel to real-scale coordinates is required to meet the monitoring purposes. Such a conversion is performed by comparing the mean radius of the circles physically printed on the target, R (mm), to the mean identified radius considering all circles and all frames, r (pixels). The scale factor R/r (mm/pixels) is then multiplied by detected coordinates to obtain their equivalent in metric scale. The target dynamic displacement is therefore evaluated as the frame-by-frame average position of all circle centers with respect to the reference condition, set as the mean of the first 200 frames, namely the average position of the target in the first few seconds of the test.

As the chessboard is considered, the intensity gradient is used to identify twelve square corners. The algorithm adopted (Geiger et al., 2012) is robust to varying imaging conditions and fully automatic, leading to the x and y coordinates of the twelve square corners in each frame, evaluated with sub-pixel accuracy. Since the ROI is still affected by perspective distortion, a scale factor is needed, differentiating among x and y directions. First, the mean inclination among vertically and horizontally aligned corners is used to rotate the chessboard, to meet the image x and y directions. The effect of the rotation on the scale factor is supposed to be very limited, since the magnitude of the rotation is very small. Then, the scaling is performed exploiting the chessboard square sides that have in common the examined corner: the scale factor is calculated as the ratio of their known length measured on the printed target L (mm) to the average pixel distance between the corner of interest and the two adjacent ones along the considered direction (mean value over frames), l_x and l_y . The target displacement time history is thus calculated as the frame-by-frame average position of corners (each scaled separately) with respect to the reference position, computed averaging the coordinates of the target in the first 200 frames, as done for the circle detection.

3.2. Feature-point matching

A feature-point matching procedure (Lydon et al., 2019) is also implemented, selecting a ROI around bolts at the examined footbridge section with no installed targets and no perspective corrections. The method is able to detect itself distinctive points on the structure to be monitored over time, dealing alone with key-points detection, description, and matching. Features initially assessed as potential key-points but not detected in all frames are automatically

discarded, therefore the algorithm only returns the x and y coordinates of points clearly identifiable from the beginning to the end of the video. However, the scaling in case of feature-point matching is well known to be a quite delicate task. Indeed, identified features are generally small elements that occupy at most few pixels. On the other hand, when a wider object is used as reference, its measurement in pixels is to be manually performed, paying attention to potential lens and perspective distortions. An expedient to solve the problem could be that of consistently narrowing the camera field of view, enriching the pixel texture around the features being monitored. At the same time, the field of view that can be monitored by the camera is reduced. In the specific case of application, however, a single shot is used to ensure fair comparison between methods. Besides, the scale factor is evaluated exploiting an artificial target installed on the structure (the nearest to the ROI), with the aim to test the potentials of the method in the best-case scenario, regardless of scaling difficulties. After the scaling operation, the mean position of key-points (with reference to the starting condition) over frames returns the dynamic displacement of the monitored footbridge section.

4. Preliminary results and discussion

Preliminary results presented in the following do only concern vertical displacements of the section located at three-eighths of the span length, but the same considerations also apply to the other monitored sections. The jumping cadence is designed to excite a purely bending mode, hence the decision to show vertical displacements instead of horizontal ones. For instance, Fig. 2 shows the case of concentric circles. Despite the measures taken to avoid camera-shaking (positioning of the camera away from the vibrating structure and video on-off remote controller), the displacement time histories of artificial targets present a non-negligible trend. Depicted in black in Fig. 2a, the target detected motion clearly suffers from a trend growth not attributable to the structure response: as predicted, fixed targets on the ground prove to be indispensable for outdoor monitoring, as external factors out of control (e.g., wind) are extremely likely to affect results. Evaluated as discussed in Section 3, the apparent motion of a fixed target made of concentric circles (red line of Fig. 2a) is used to reconstruct the actual displacement of the structure, leading in the example case to the structural dynamic displacement illustrated in black in Fig. 2b. For validation purposes, vision-based displacements are compared to those derived by double integrating the accelerometer recordings (blue line in Fig. 2b). Specifically, displacement time series are reconstructed from the measured accelerations by adopting a method that combines Tikhonov regularization and an overlapping time window (Lee et al., 2010), which has proven to be accurate and efficient for the reconstruction of dynamic displacements in low frequency dominant structures. As concentric circles are referred, the time-domain comparison between vision-based and traditional monitoring is shown in Fig. 2b, revealing a good correspondence but also remarkable differences. As concerns the noise level, the standard deviation of displacements in ambient condition (period prior to jumping excitation) obtained by the vision-based technique is 0.22 mm, while that derived by accelerations is 0.05 mm.

If the same procedure is carried out not considering all concentric circles but only one (e.g., the outermost) in both moving and fixed targets (black and red lines of Fig. 3a, respectively), the benefit of averaging multiple detections is lost, resulting in less accurate and more noisy actual displacements (black line of Fig. 3b). In the example section, the actual displacement standard deviation in undisturbed condition is almost tripled from 0.22 (concentric circles) to 0.67 mm (outermost circle alone), quantitatively demonstrating the greater robustness of concentric circles with respect to one. As regards chessboard tracking, detected, apparent, and actual displacements are depicted in Fig. 4a and Fig. 4b, together with traditional monitoring results. The ambient standard deviation of actual vision-based displacements is 0.07 mm, noise performance value quite comparable to that obtained by extracting displacements from accelerations, and one third of the standard deviation obtained with concentric circles. This reveals that, among the selected target geometries, the chessboard is perhaps the most suitable for monitoring purposes. And this despite the fact the designed chessboard tracking algorithm is independent from image perspective distortions, in contrast with the developed circle shape detection procedure.

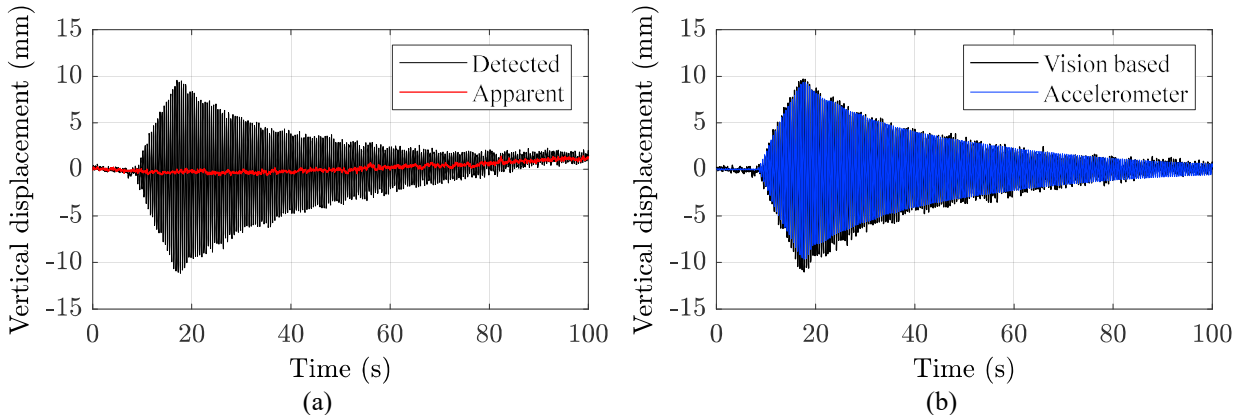


Fig. 2. Concentric circles at three-eighths section: (a) detected displacement of the target on the structure and apparent displacement of the target at the ground; (b) vision-based actual displacement derived by subtraction and displacement reconstructed from measured accelerations.

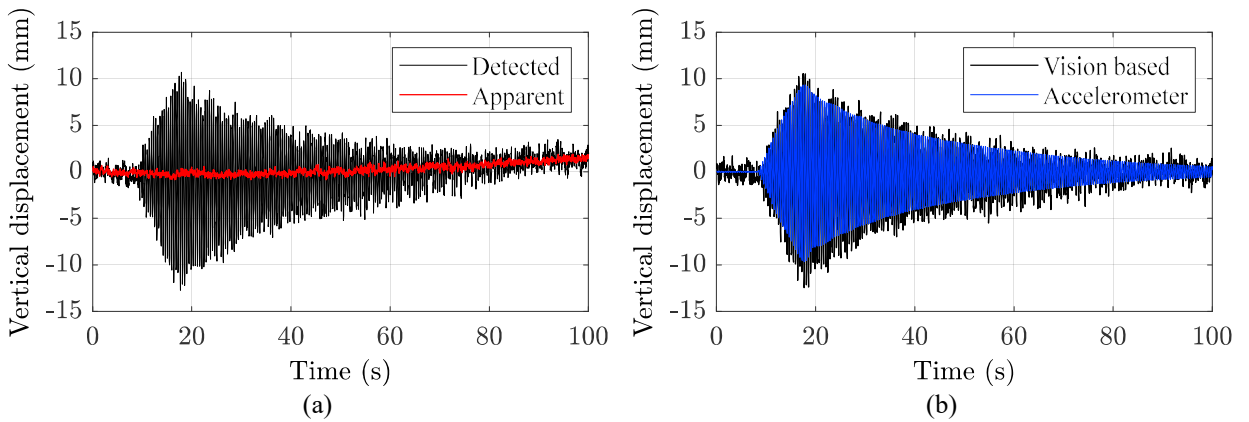


Fig. 3. Outermost circle at three-eighths section: (a) detected displacement of the target on the structure and apparent displacement of the target at the ground; (b) vision-based actual displacement derived by subtraction and displacement reconstructed from measured accelerations.

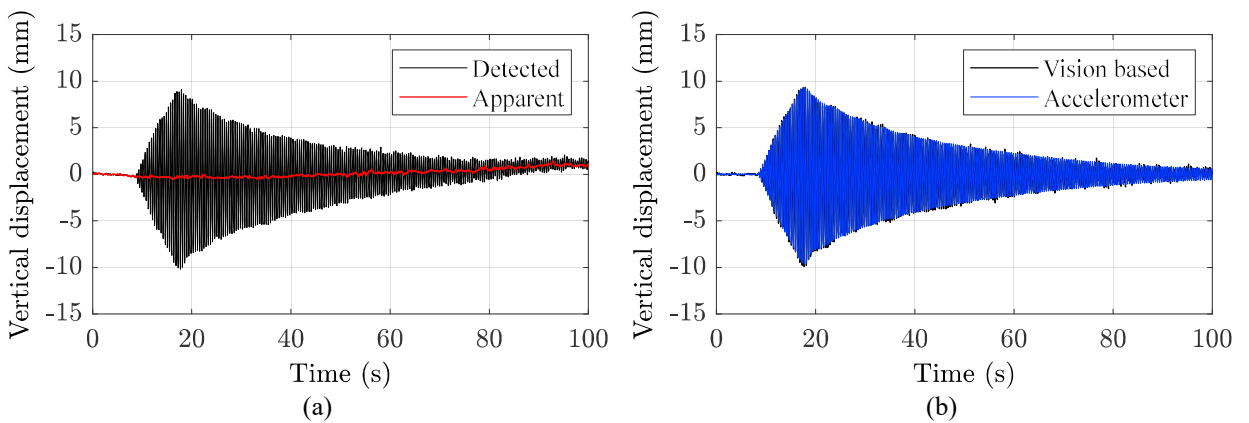


Fig. 4. Chessboard at three-eighths section: (a) detected displacement of the target on the structure and apparent displacement of the target at the ground; (b) vision-based actual displacement derived by subtraction and displacement reconstructed from measured accelerations.

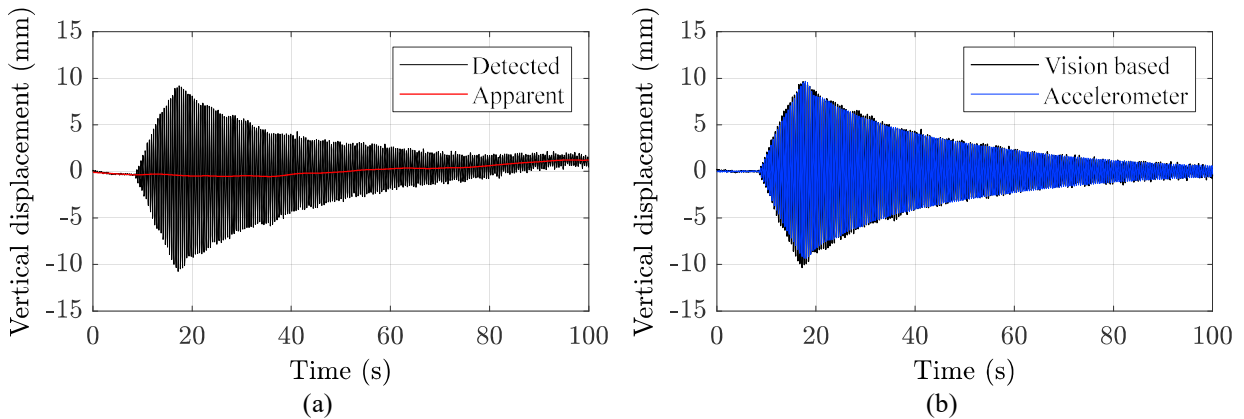


Fig. 5. Feature-point matching at three-eighths section: (a) detected displacement of structural bolts and apparent displacement from singular spectral analysis; (b) vision-based actual displacement derived by subtraction and displacement reconstructed from measured accelerations.

Dynamic displacements obtained by the feature-point matching algorithm of Leutenegger et al. (2011) are shown in black Fig. 5a. Beside the delicate scaling (here fixed by exploiting artificial targets), another difficulty lies in the definition of the structure apparent motion. Indeed, in the application case, if targets on the ground had not been foreseen, there would have been no fixed objects to be tracked with the feature-point matching algorithm itself, due to the dense vegetation. To obtain results in the best-case scenario, the camera motion is therefore calculated using the singular spectrum analysis (Golyandina and Zhigljavsky, 2013). The latter performs a decomposition of the detected displacement time series, identifying the long-term trend, the oscillatory components, and the remainder. Thereby it is possible to distinguish between the apparent (red line of Fig. 5a) and actual (black line of Fig. 5b) movements of the structure section. A remarkable drawback of this approach is the impossibility of detecting and separating permanent displacements due to damage from the apparent motion caused by camera vibration. In so doing, the ambient standard deviation of actual displacements turns 0.12 mm, quite in line with the proposed algorithms for both circle and chessboard tracking. However, in real case applications, aspects here neglected could strongly affect results. Above all, a stationary object should be identified or provided in advance to reach potentially higher accuracies. Besides, the smaller the target within the same image, the more delicate the scaling. This implies that, with respect to artificial target tracking, accurate scaling with feature-point matching generally requires a narrower field of view with the same resolution. However, this might be a severe drawback when multiple sections are monitored: each of them might necessitate its own camera, introducing the need for camera synchronization as well as additional instrument and computational costs.

5. Conclusions and future perspectives

With the aim of detecting vertical dynamic displacements on large-scale structures, two vision-based procedures based on circle and chessboard tracking are set up and tested on a real case study. The latter consists in a highly deformable footbridge, equipped with artificial targets placed in several strategic sections. Videos are acquired by using a consumer-grade camera placed on the riverbed. However, the procedure could be either adopted placing the camera on the riverside, as demonstrated in Buoli et al., 2023. As expected, on-site camera shaking due to unmanageable external factors is not negligible. This implies the need for fixed targets, whose apparent motion is essential to clean the structural time history from the unknown camera movement. The comparison between the designed vision-based methods and a traditional monitoring system returns a not complete but satisfying match, especially considering the consistent saving in terms of installation time and costs. Diverse target patterns are tested. Concentric circles show an almost tripled accuracy with respect to a single one, demonstrating that the possibility of averaging multiple detections within the same frame strictly affects the robustness of vision-based results. The chessboard reveals high accuracy independently of the perspective correction, achieving an ambient noise which is strictly comparable to traditional monitoring. A feature-point matching algorithm proposed in literature is also

implemented, revealing – in favorable cases – accuracies quite similar to the proposed target tracking procedures. However, difficulties in apparent motion identification and scaling could be a discriminating factor in real conditions. The application presented consists in a dynamic monitoring, but all the approaches can potentially be applied to also detect long-term static displacements. Besides camera shaking and target geometry, which are herein deepened, future studies could be aimed at exploring the impact of other uncertainty sources on the proposed methods, such as lighting, field of view, or resolution.

6. Acknowledgements

This work was supported by the FAR Mission Oriented 2023 Project (Vision-based approaches for the structural health monitoring of existing bridges, VIS4SHM). The financial support of the University of Modena and Reggio Emilia and the “Fondazione di Modena” is gratefully acknowledged.

References

- Atherton, T. J., Kerbyson, D. J., 1999. Size invariant circle detection. *Image and Vision computing* 17(11), 795-803.
- Bassoli, E., Vincenzi, L., Grassi, F., Mancini, F., 2023. A multi-temporal DInSAR-based method for the assessment of the 3D rigid motion of buildings and corresponding uncertainties. *Journal of Building Engineering* 73, 106738.
- Buoli, E., Bassoli, E., Eslami Varzaneh, G., Ponsi, F., Vincenzi, L., 2023. Vision-based dynamic monitoring of a steel footbridge. *Proceedings of the XII International Conference on Structural Dynamics*, Delft, The Netherlands.
- Castagnetti, C., Bassoli, E., Vincenzi, L., Mancini, F. 2019. Dynamic assessment of masonry towers based on terrestrial radar interferometer and accelerometers *Sensors (Switzerland)* 19(6), art. no. 1319.
- Chen, J. G., Adams, T. M., Sun, H., Bell, E. S., Büyüköztürk, O., 2018. Camera-based vibration measurement of the world war I memorial bridge in Portsmouth, New Hampshire. *Journal of Structural Engineering* 144(11), 04018207.
- Comanducci, G., Magalhães, F., Ubertini, F., Cunha, Á., 2016. On vibration-based damage detection by multivariate statistical techniques: Application to a long-span arch bridge. *Structural health monitoring* 15(5), 505-524.
- Dong, C. Z., Bas, S., Catbas, F. N., 2020. Investigation of vibration serviceability of a footbridge using computer vision-based methods. *Engineering Structures* 224, 111224.
- Dong, C.Z., Catbas, F. N., 2020. A review of computer vision-based structural health monitoring at local and global levels. *Structural Health Monitoring* 20(2), 692-743.
- Feng, D., Feng, M. Q., 2017. Experimental validation of cost-effective vision-based structural health monitoring. *Mechanical Systems and Signal Processing* 88, 199-211.
- Fradelos, Y., Thalla, O., Biliani, I., Stiros, S., 2020. Study of lateral displacements and the natural frequency of a pedestrian bridge using low-cost cameras. *Sensors* 20(11), 3217.
- Geiger, A., Moosmann, F., Car, Ö., Schuster, B., 2012. Automatic camera and range sensor calibration using a single shot. *IEEE international conference on robotics and automation*, pp. 3936-3943.
- Golyandina, N., Zhigljavsky, A., 2013. *Singular Spectrum Analysis for Time Series*. SpringerBriefs in Statistics. Berlin, Heidelberg: Springer Berlin Heidelberg.
- Guerzoni, G., Faghand, E., Vitetta, G.M., Vincenzi, L., Mehrshahi, E. (2023) Novel Movement-Based Methods for the Calibration of Colocated Multiple-Input Multiple-Output Radars, *IEEE Access*, in printing.
- Guidorzi, R., Diversi, R., Vincenzi, L., Simioli, V., 2010. MEMS-based sensing for health monitoring of buildings. *Fifth European Workshop on Structural Health Monitoring*, pp. 901-906.
- Lee, H. S., Hong, Y. H., Park, H. W., 2010. Design of an FIR filter for the displacement reconstruction using measured acceleration in low-frequency dominant structures. *International Journal for Numerical Methods in Engineering* 82(4), 403-434.
- Lee, J., Lee, K. C., Jeong, S., Lee, Y. J., Sim, S. H., 2020. Long-term displacement measurement of full-scale bridges using camera ego-motion compensation. *Mechanical Systems and Signal Processing* 140, 106651.
- Leutenegger, S., Chli M., Siegwart, R. Y., 2011. BRISK: Binary Robust invariant scalable keypoints. *International Conference on Computer Vision*. Barcelona, Spain, pp. 2548-2555
- Lydon, D., Lydon, M., Taylor, S., Del Rincon, J. M., Hester, D., Brownjohn, J., 2019. Development and field testing of a vision-based displacement system using a low cost wireless action camera. *Mechanical Systems and Signal Processing* 121, 343-358.
- Poluzzi, L., Barbarella, M., Tavasci, L., Gandolfi, S., Cenni, N. 2019. Monitoring of the Garisenda Tower through GNSS using advanced approaches toward the frame of reference stations, *Journal of Cultural Heritage* 38, 231-241.
- Ponsi, F., Bassoli, E., Vincenzi, L., 2022. Bayesian and deterministic surrogate-assisted approaches for model updating of historical masonry towers. *Journal of Civil Structural Health Monitoring* 12(6), 1469-1492.
- Ponsi, F., Bassoli, E., Vincenzi, L., 2023. Mitigation of model error effects in neural network-based structural damage detection. *Frontiers in Built Environment*, 8.
- Ranieri, C., Notarangelo, M. A., Fabbrocino, G., 2020. Experiences of Dynamic Identification and Monitoring of Bridges in Serviceability Conditions and after Hazardous Events. *Infrastructures* 5(10), 86.

- Spencer, B.F., Hoskere, V., Narazaki, Y., 2019. Advances in computer vision-based civil infrastructure inspection and monitoring. *Engineering* 5(2), 199-222.
- The MathWorks, Inc. MATLAB Image Processing and Computer Vision Toolbox Release 2022b. Natick, Massachusetts, United States.
- Xu, Y., Brownjohn, J. M., Huseynov, F., 2019. Accurate deformation monitoring on bridge structures using a cost-effective sensing system combined with a camera and accelerometers: Case study. *Journal of Bridge Engineering* 24(1), 05018014.
- Xu, Y., Brownjohn, J., Kong, D., 2018. A non-contact vision-based system for multipoint displacement monitoring in a cable-stayed footbridge. *Structural Control and Health Monitoring* 25(5), e2155.
- Ye, X. W., Yi, T. H., Dong, C. Z., Liu, T., 2016. Vision-based structural displacement measurement: System performance evaluation and influence factor analysis. *Measurement* 88, 372-384.
- Zona, A., 2020. Vision-based vibration monitoring of structures and infrastructures: An overview of recent applications. *Infrastructures* 6(1), 4.